ARTICLE IN PRESS

Available online at www.sciencedirect.com

SciVerse ScienceDirect

Scripta Materialia xxx (2012) xxx–xxx

Scripta MATERIALIA

www.elsevier.com/locate/scriptamat

On the dynamic character of localized failure

S. Osovski,[a,*] Y. Nahmany,[a] D. Rittel,[a] P. Landau[b] and A. Venkert[b]

[a]*Faculty of Mechanical Engineering, Technion, 32000 Haifa, Israel*
[b]*Department of Physics, NRCN, Beer-Sheva 84190, Israel*

Received 19 March 2012; revised 29 June 2012; accepted 2 July 2012

The dynamic stored energy of cold work (SECW) has recently been identified as the trigger for adiabatic shear failure. However, the question of what makes the failure "dynamic" has remained open so far. Using compression tests (Ti6A14V alloy) over a wide range of strain rates [10^{-4}–10^{4} s^{-1}], we have identified a transition strain rate above which both the dynamic SECW and the microstructure are radically different from their static counterparts, thereby outlining the onset of "dynamic" failure.
© 2012 Acta Materialia Inc. Published by Elsevier Ltd. All rights reserved.

Keywords: Shear bands; Microstructure; Dynamic recrystallization; Transmission electron microscopy (TEM)

Dynamic shear localization is known to be a major failure mechanism under dynamic loading conditions. It is well accepted that the source of dynamic shear localization is the growth of some initial heterogeneity, the exact nature of which is not well identified. The traditional approach is based on the work of Zener and Hollomon [1], who suggested that the inherent temperature rise during dynamic (and therefore adiabatic) loading can cause material softening, leading eventually to strain localization (see also [2,3]). Recently, it was shown by Rittel et al. [4–6] that the commonly accepted thermal softening approach may be replaced by a microstructural one, suggesting that dynamic shear failure of crystalline solids can be initiated by local microstructural changes (dynamic recrystallization, DRX) [7,8]. Furthermore, it was identified that the driving force for the microstructural evolution leading to DRX is the dynamic stored energy of cold work (SECW) [5]. These authors reported that quasi-static cold work has little effect, if any, on the amount of dynamic work needed to cause subsequent dynamic shear localization and failure. One point which was not addressed in Ref. [5] concerns the exact nature and meaning of the term "dynamic" in this context. In other words, what makes dynamic failure really dynamic is currently undefined. In this work we attempt to supply an experimental answer to the above-stated question, based on dynamically stored energy considerations.

Since energy storage has been identified as the trigger for dynamic shear failure through DRX formation [6,9], we performed here a set of compression tests at strain rates ranging from 10^{-4} [s^{-1}] to 10^{4} [s^{-1}], and measured the total amount of mechanical work needed in order to bring the specimen to failure, i.e. the dynamic deformation energy. The latter comprises the dynamic SECW and the reversible elastic strain energy density. In order to determine the dynamic SECW from the dynamic deformation energy, one must know the Taylor–Quinney coefficient precisely [10]. Since the elastic part of the dynamic deformation energy is quite small with respect to the SECW, however, mostly at large strains, the total deformation energy is used here, as it was in our previous work [5]. Following the mechanical experiments, representative specimens from selected strain rates were investigated using transmission electron microscopy in order to detect the presence of dynamically recrystallized nano grains, based on the premise that DRX means dynamic shear localization.

All the mechanical tests were performed using a shear compression specimen (SCS) [11] in which the failure locus is predetermined by the existence of a geometrical stress concentration in the fillet.

Dynamic compression tests (10^{2}–10^{4} [s^{-1}]) were performed usinga Kolsky bar (SPHB) [12], while static compression experiments (10^{-3}–10^{0} [s^{-1}]) were conducted on a servo-hydraulic testing machine (MTS 810). The tested material was chosen to be Ti6Al4V

* Corresponding author. Tel.: +972 523466185; e-mail: shmulo@gmail.com

1359-6462/$ - see front matter © 2012 Acta Materialia Inc. Published by Elsevier Ltd. All rights reserved.
http://dx.doi.org/10.1016/j.scriptamat.2012.07.001

alloy in the annealed condition with an average grain size of 10 μm.

Figure 1 present typical stress–strain curves obtained for both dynamic and quasi-static loading.

While strain rates of (10^3–10^4 [s^{-1}]) are easily obtained using the SPHB, in order to obtain results at strain rates of the order of 10^2 [s^{-1}] it was necessary to perform a series of interrupted experiments for each specimen, using maraging steel stop rings which allow the controlled application of strains to the specimen. In those experiments, the specimen experienced slightly different strain rates at each loading step. Typical stress–strain curves for strain rates of the order of 10^2 [s^{-1}] are presented in Figure 2, in which the range of applied strain rates was within 350–550 s^{-1}.

The deformation energy (static and dynamic, W_{mec}) was calculated for each experiment using Eq. (1):

$$W_{mec} = \int_0^{\varepsilon_f} \sigma d\varepsilon_p \tag{1}$$

with σ being the Mises stress, ε_p the plastic strain and ε_f the failure strain. The deformation energy invested up to failure is plotted in Figure 3 as a function of $\log(\dot{\varepsilon})$. From Figure 3, the existence of a transition strain rate from static to dynamic is obvious at $\dot{\varepsilon} \approx 10^2$ [s^{-1}].

To better understand this result, specimens deformed at representative strain rates were examined in a Jeol 300 transmission electron microscope (marked in Fig. 3). All specimens deformed in the high strain rate regime, $\dot{\varepsilon} \geq 10^3$ [s^{-1}], showed dynamically recrystallized grains of the order of a few tens of nanometers within the localized band. By contrast, specimens deformed in the quasi-static regime did not exhibit DRX at all. Some of the specimens that were deformed in the transitional strain rates of 10^2–10^3[s^{-1}] displayed DRX, while others did not. Since the loading rate of these specimens varied at each step, as mentioned above, it was not possible to accurately pinpoint the transition strain rate. Consequently, while the transition is well marked in Figure 3, the results in the transition domain are quite scattered in terms of deformation energy. Finally, it should be noted that the dynamic deformation energy remains remarkably constant in the strain rate range of 1000–13000 s^{-1}. This observation has not been reported before, and may considerably simplify numerical models of dynamic shear localization where a wide range of strain rates is typically involved, as in Dolinsky et al. [13].

The phenomenon of dynamic shear localization is often referred to in the literature as adiabatic shear banding, implying that high strain rate deformation is adiabatic in nature [10]. Looking at the results presented in Figure 3 with the adiabatic nature of the process in mind, one might suspect that the observed transitional strain rate simply reflects the transition from an isothermal to an adiabatic deformation regime. In order to

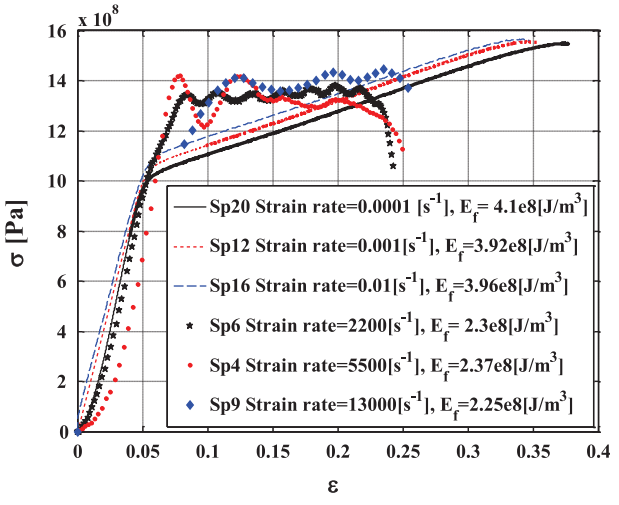

Figure 1. Experimental stress–strain curves at different loading rates, as measured on SCSs. All curves are plotted up to failure.

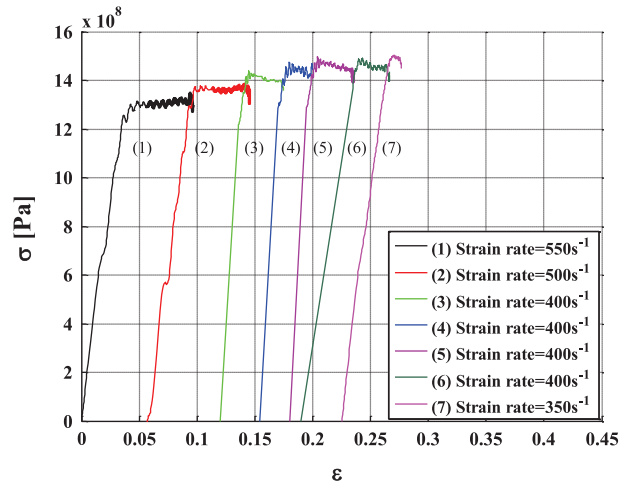

Figure 2. Composite stress–strain curve measured on an SCS using multiple loading intervals, with $\dot{\varepsilon}$ in the range of 350–550 s^{-1}.

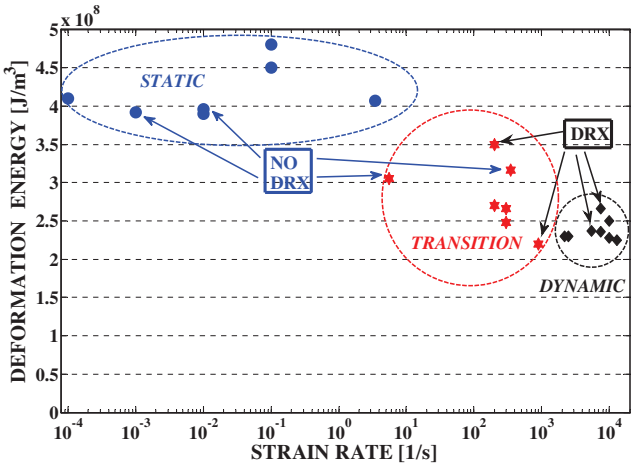

Figure 3. Deformation energy until failure (static and dynamic) as a function of the strain rate. A transition is clearly seen around 10^2 [s^{-1}]. Specific specimens that were examined under TEM are arrowed, as representatives of their group of strain rates. Note the three distinct regions: blue: high energy values and no DRX (at all); black: low energy values and DRX in all specimens; and red: a transition regime where the energies are scattered between the two values while DRX is observed for some specimens only (For interpretation of the references to color in this figure legend, the reader is referred to the web version of this article.).

refute this possibility, experiments were performed at strain rates higher than the apparent transitional strain rate, in which the specimen was deformed incrementally to failure in a few steps, each step being followed by a pause to allow for cooling. Due to the small increment of strain imparted to the specimen, these tests can be considered as quasi-isothermal. The dynamic deformation energy until failure was calculated for these quasi-isothermal tests, and was found to be similar to that measured for uninterrupted dynamic experiments. Note that similar tests were reported for Ti6Al4V in Ref. [14].

At this stage, one should note that, while the dynamically stored energy of cold work has been identified as the key factor driving microstructural changes [5], we consider here the total mechanical energy, which includes both the stored and dissipated components. The results presented in this work demonstrate that, in order to address dynamic shear localization, one has to consider the effect of strain rate on the evolution of the microstructure. By identifying the rate controlling mechanism (e.g. cross slip, recovery) that determines the minimal strain rate leading to DRX and subsequent shear localization, one should be able to better choose and even design materials with a higher resistance to dynamic shear failure. In this respect, it would be desirable to develop a deeper understanding of the link between the microstructural and mechanical observations reported in this and similar works [5,6,15]. For this, one would need to identify the rate- and mechanism-controlling parameters, e.g. in the way shown by Landau et al. [16], who combined TEM observations and atomistic calculations to quantify the cross-slip activation energy. However, this is only one of the factors that could lead to microstructural refinement, and additional work in this direction is still needed.

The authors thank Dr. E. Bouchbinder for helpful discussions. The support of Israel Science Foundation (Grant 2011362) is gratefully acknowledged.

[1] C. Zener, J.H. Hollomon, J. Applied Phys. 15 (1944) 22.
[2] Y. Bai, B. Dodd, Shear Localization: Occurrence, Theories, and Applications, Pergamon Press, Oxford, 1992.
[3] T. Wright, The Physics and Mathematics of Adiabatic Shear Bands, Cambridge University Press, Cambridge, 2002.
[4] D. Rittel, Z.G. Wang, Mech. Mater. 40 (2008) 629.
[5] D. Rittel, Z.G. Wang, M. Merzer, Phys. Rev. Lett. 96 (2006) 075502.
[6] D. Rittel, P. Landau, A. Venkert, Phys. Rev. Lett. 101 (2008) 165501.
[7] U. Andrade, M.A. Meyers, A.H. Chokshi, Scripta Metall. Mater. 30 (1994) 933.
[8] M.A. Meyers, J.C. LaSalvia, V.F. Nesterenko, Y.J. Chen, B.K. Kad, in: T.R. McNelley (Ed.), The Third International Conference on Recrystallization and Related Phenomena, MIAS, 1996, pp. 279.
[9] P. Landau, A. Venkert, D. Rittel, Metall. Mater. Trans. A 41 (2010) 389.
[10] G.I. Taylor, H. Quinney, Proc. Royal Soc. Lond. 143 (1934) 307.
[11] D. Rittel, S. Lee, G. Ravichandran, Exp. Mech. 42 (2002) 58.
[12] H. Kolsky, Proc. Phys. Soc. Lond. 62 (B) (1949) 676.
[13] M. Dolinsky, D. Rittel, A. Dorogoy, J. Mech. Phys. Solids 58 (2010) 1759.
[14] D. Rittel, Z.G. Wang, A. Dorogoy, Int. J. Impact Eng. 35 (11) (2008) 1280.
[15] S. Osovski, D. Rittel, P. Landau, A. Venkert, Scripta Mater. 66 (2012) 9.
[16] P. Landau, D. Mordehai, A. Venkert, G. Makov, Scripta Mater. 66 (2012) 135.